Experiments in Fluids 32 (2002) 674–682 © Springer-Verlag 2002
DOI 10.1007/s00348-002-0415-x

Flow regime identification in a two-phase flow using wavelet transform

T. Elperin, M. Klochko

Abstract This study addresses the problem of the automatic flow regime identification in two-phase flows in pipes. A novel wavelet transform-based approach is proposed and validated using time series of differential pressure fluctuations. The experimental data on the differential pressure measured in a vertically installed Venturi meter for air–water flow were analyzed and found to be appropriate for flow regime identification. The wavelet spectrum of the measured signal is shown to characterize the flow patterns completely, and the vector of the wavelet variances is proposed as the characteristic vector for use in an on-line flow regime identification system.

1 Introduction

The most characteristic feature of two-phase mixture flows in pipes is their ability to acquire various spatial distributions of phases known as the flow patterns. The generally accepted classification differentiates three basic flow patterns in vertical pipes: bubbly flow with one fluid dispersed as discrete bubbles in a continuous second fluid; annular flow, when one fluid flows as a thin film on the wall and the second as a core at the center of the pipe; intermittent flow with non-uniform distribution of fluids along a pipe. Each flow pattern has an intrinsic hydrodynamics governing the behavior of many flow parameters, such as pressure drop, gas void fraction, as well as heat and mass transfer. Therefore, it is of crucial importance in the modeling and operation of two-phase flow systems to know the instantaneous flow pattern. Several methods exist for detecting a particular flow regime. Two-phase flow regime maps which are plotted by correlating a set of experimental data represent the flow regime boundaries as a function of hydrodynamic flow parameters and fluids properties. The generalization of the flow regime maps is an almost unfeasible task, since there are many parameters governing the transition between flow regimes, and hence, their application is restricted to the conditions covered by experimental data set. Another approach is modeling of the transition boundaries between the flow regime, which implies identification of the transition mechanism for each pair of flow patterns (see, e.g., Taitel 1990). Such models usually incorporate all the relevant flow parameters and, therefore, are applicable for different flow conditions. However, the application of the models implies that the flow is steady and developed, which is rarely attainable in practice. Additional shortcomings of both flow regime differentiation methods is that they require a priori knowledge of the flow parameters and are not reliable when the flow conditions are close to the transition boundaries between flow regimes.

Flow pattern identification can be performed either by visual inspection of the flow in a transparent pipe or by measuring and quantifying fluctuations of the natural flow parameters such as gas void fraction (Jones and Zuber 1975; Barnea et al. 1980; Vince and Lahey 1982; Costigan and Whalley 1997; Tsoukalas et al. 1997) or differential pressure (Tutu 1982; Matsui 1984, 1986), which are supposed to reflect the flow configuration. The second approach is basically the statistical pattern recognition problem, which is somewhat simplified by the fact that these fluctuations can be modeled or at least described heuristically, depending upon the flow regime, since the waveform of the signal is closely related to the spatial distribution of the flowing phases.

A variety of techniques proposed for automatic flow regime identification make use of the peak values and shape characteristics of the probability density function (PDF) or power spectral density function (PSD) of the measured time series. It has been shown that the PDFs for bubbly and annular flows exhibit a single peak corresponding to the low and high gas void fraction, respectively, whereas slug flow is characterized by a bimodal PDF with a low-void peak corresponding to the liquid slug passage and a high-void peak due to the Taylor bubble. The spectral analysis of the measured signals revealed three types of PSD: a wide-band low-amplitude spectrum associated with bubbly flows, a low frequency peak of large amplitude corresponding to the characteristic frequency of slug flow, and a medium-width band spectrum for annular flow. However, it has been shown (Vince and Lahey 1982) that the moments of the PSD, except for the variance, depend on the liquid phase superficial velocity and, consequently, their use for flow regime identification requires knowledge of the liquid flow rate.

Received: 7 November 2001 / Accepted: 21 January 2002
Published online: 17 April 2002

T. Elperin (✉), M. Klochko
The Pearlstone Center for Aeronautical Engineering Studies
Department of Mechanical Engineering
Ben-Gurion University of the Negev
PO Box 653, Beer Sheva, 84105, Israel
E-mail: elperin@menix.bgu.ac.il

This study was supported by Agar Corporation (Houston, TX, USA). We are grateful to Jo Agar, David Farchi and the staff of the Agar Corporation for the help in conducting the experiments and for useful discussions.

Franca et al. (1991) and Cai et al. (1996) studied the application of fractal techniques for flow regime identification and asserted that the fractal dimension of the pressure signal embedded into a pseudo-phase space carries the information associated with the flow regime. Soldati et al. (1996) applied diffusional analysis to the measured signals of gas void fraction, liquid holdup and pressure drop. In the latter study, it was found that the short- and long-term correlation properties of the mean square displacement of the diffusion process generated from the experimental time series are closely related to the flow regime and, moreover, it was found that the results are almost independent of the measuring scheme. Later observation confirms once more the possibility of flow regime identification using fluctuations of any flow parameter related to the gas void fraction. However, calculating the fractal dimension or scaling exponent of a diffusion process is tedious and time consuming, which prevents the practical application of these methods.

All the aforementioned methods for flow pattern recognition rely on various statistical properties of the signal waveform in the time, frequency or pseudo-phase domain. Hence, in order to obtain reliable results, the analyzed signal must have sufficient length to yield statistically significant estimates of the characteristic parameters. This imposes the additional restriction on the stability of the flow which makes these methods appropriate for laboratory tests, for constructing flow regime maps, etc., but none of them can provide information about the instantaneous state of the flow in the on-line mode. In addition, the flow structure is highly unstable in the vicinity of the transition between flow regimes, and patterns characteristic of different regimes can alternate along a pipe, which makes objective flow regime identification very difficult. Therefore, it is desirable to identify the flow regime using a short-length signal.

In the present study, we investigate the applicability of a promising new approach to flow pattern classification based on the wavelet transform, which has been widely used in signal processing and analysis and showed itself to be the superior tool for the analysis of non-stationary and transient signals due to its localization properties in the time domain. Moreover, the localization of the wavelets in the frequency domain means that the wavelet transform coefficients incorporate features of the PSD and, consequently, can be used for flow regime identification. These anticipations were validated by Kirpalani et al. (2001), who applied the continuous wavelet transform to the analysis of time series of wall pressure fluctuations in various two-phase flow regimes. They found that the wavelet spectrum of the measured signal possesses features that are similar to the PSD of the wall pressure time series reported by Hubbard and Dukler (1966).

The method proposed in this study was verified using the experimental time series of the differential pressure through a Venturi tube. Such arrangement of the test section permits flow regime identification simultaneously with the flow measurement procedure and, moreover, demonstrates that the method developed can be easily implemented for use with any measuring scheme provided its input is related to the gas void fraction.

2 Experimental setup

2.1 Test loop

Experiments on two-phase flow pattern recognition were carried out using a multiphase flow facility at the Agar Corporation (Houston, USA). Liquids and air were pumped separately through the metering devices before mixing. The gas flow metering block consists of four rotameters with various overlapping ranges for measuring small flow rates, and two vortex meters with a velocity measurement range of 2–76 m/s. The vortex meters were installed in pipes with different diameters thus allowing two different volume flow rate ranges to be obtained. All these devices were installed in parallel and activated by block valve switching. The liquid flow rate was measured by an electromagnetic flow meter with a flow range of 20–650 l/min, and by a positive displacement flow meter (250–8,000 l/min) installed in series. The use of multiple flow meters allowed the turn-down ratio of the controlling equipment to be increased. Flow rate regulation in both lines was performed by control valves. Air and tap water were used as the working fluids in the flow pattern recognition experiments.

Water was mixed with air coming from the gas line, and the two-phase mixture flowed through a horizontal pipe with an inner diameter equal to that of the test section. Then the mixture passed through the test section, and flowed into the liquid tank, where air was separated and vented to the atmosphere.

The vertical test section (see Fig. 1) comprises a transparent Plexiglas Venturi meter with a 3-in. inlet and a 1.5-in. throat nominal diameters (72.4 and 38.1 mm i.d., respectively). The transparency of the Venturi tube

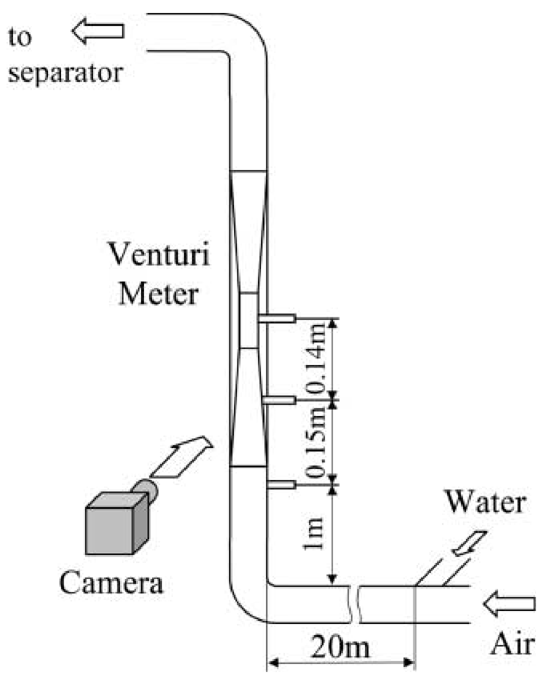

Fig. 1. Scheme of the test section

afforded visual observations of the flow patterns to be carried out. The fast-response piezoresistive Omega PX236 pressure transducers (range 0–30 psig, response time 1 ms) were located before the inlet, at the middle of the converging part and at the throat of the Venturi meter. The calibration detected a minimal signal-to-noise ratio (SNR) of 5 during the single-phase liquid flow at the lower flow rate ($6\times10^{-4} m^3/s$). In this case, the flow was laminar, and the signal was much weaker than is expected in a two-phase flow owing to the gas void fraction fluctuations and, therefore, the SNR in two-phase flow runs was much higher.

The pressure signals were sampled at a frequency of 1,250 Hz and recorded using the acquisition board UPC-500 to the personal computer. In order to reduce the interchannel sampling delay in calculating the differential pressure, every four pressure readings were averaged prior to converting, thus yielding the effective sampling frequency of 312.5 Hz. It was shown in earlier studies (e.g., Cai et al. 1996) and confirmed by our preliminary tests that the pressure signal contains negligible energy at frequencies greater than 100 Hz, even at the highest flow rates of fluids, which is lower than the Nyquist frequency in our experiment. The pressure time series were registered for 60 s for each run simultaneously with the flow image, which was recorded by means of a camcorder.

The measured signals, i.e., inlet p_i, middle p_m, and throat p_t pressures, were subtracted, and the resulting differential pressure time series $\Delta p_1=p_i-p_m$ and $\Delta p_2=p_i-p_t$ were processed using MATLAB (The MathWorks, Inc., Mass., USA) software. It will be shown further that the high-frequency content of the signal is the main characteristic of some flow regimes and, accordingly, we did not perform any filtering besides the signal averaging prior to sampling.

2.2 Flow conditions

The goal of the present study was to develop a flow regime identification method which is insensitive to flow unsteadiness and transients. Hence, no special care was taken during the experiments to ensure either a particular flow regime in the test section or a developed steady-state flow. This provided the feasibility of investigating flow patterns in unsteady and undeveloped flows where no definite flow state can be matched to a pair of phase flow rates. Such a situation is common for multiphase flow systems, where flows are seldom stable and developed. That is also the reason why no special gas–liquid mixing procedure was provided and also why the entrance section before the test section was relatively short.

The only parameters controlled and kept constant during each experimental run were the fluids flow rates, varied in the wide range – 6×10^{-4} to 1.3×10^{-2} m^3/s for water and 0–0.02 m^3/s for air.

3 Experimental results

The analysis of the measured time series of dynamic pressure fluctuations showed that they contain information originating mostly outside the test section, e.g., fluctuations from pumps, flow loop vibrations, etc., and it was almost impossible to detect the fluctuations related to the flow regime even by visual inspection. In order to eliminate such irrelevant influence, the differential pressures through a test section must be calculated (see, e.g., Tutu 1982; Matsui 1984). We chose the differential pressure through the Venturi meter as the basis for the pattern recognition method for two reasons. First, Venturi meters are widely used in the multiphase flow metering systems and, therefore, the flow regime identification can be performed simultaneously with the measuring process. The second reason is that the acceleration of the flow in a Venturi causes an increase in the signal sensitivity to the void fraction fluctuations due to the large difference in the densities of air and water.

Inspecting the recorded video images of the two-phase flow through the Venturi meter, we found that the flow structures, such as liquid film and large bubbles, are stable during the flow through the convergent section and break up in the divergent section of the Venturi. Thus, the differential pressure signal measured between the inlet and throat of the Venturi meter reflects the processes characteristic of a particular flow regime, which allows us to use this signal in developing the flow regime identification method. This very special measurement scheme, however, does not restrict the application of the method developed, and it can be generalized to the analysis of measurements of the differential pressure in a straight pipe or direct void fraction measurements.

The visual comparison as well as the wavelet spectrum calculations (see Sect. 5) for the two time series Δp_1 and Δp_2 revealed that they exhibited very similar responses to a particular flow pattern with two minor differences. The Δp_2 signal featured greater amplitude fluctuations due to the greater ratio of the cross-section areas (stronger flow acceleration in the second half of the converging cone). In contrast, Δp_1 exhibited a clearer response to the small flow structures, such as short-length Taylor bubbles or liquid bridges, due to the smaller distance between the pressure transducers. The dependence of the differential pressure signal waveform characteristics on the distance between pressure transducers was noted in several previous studies (see, e.g., Matsui 1984). The reason is that the differential pressure in a vertical two-phase flow represents the mean volumetric void fraction in the pipe section between transducers rather than the cross-section average provided by the direct void fraction measurements. Hence, we have chosen the differential pressure $\Delta p_1=p_1-p_m$ between the inlet and the middle of the converging part of the Venturi meter in the present study because of its better sensitivity to the smaller flow structures.

Figures 2, 3, 4 and 5 show the typical differential pressure time series Δp_1 for basic flow regimes occurring in the two-phase flow in vertical pipes. The corresponding averaged superficial velocities of air and water at the inlet conditions are presented in Table 1.

In a bubbly flow, the gas phase is almost uniformly distributed as discrete bubbles in a continuous liquid, and the corresponding signal (Fig. 2) resembles quasi-stationary high-frequency noise.

Table 1. Averaged water and air superficial velocities at the Venturi inlet conditions for the time series presented in Figs. 2, 3, 4 and 5

Time series	Bubbly flow (Fig. 2)		Annular flow (Fig. 3)		Slug flow (Fig. 4)		Churn flow (Fig. 5)	
	U_L (m/s)	U_G (m/s)	U_L (m/s)	U_G (m/s)	U_L (m/s)	U_G (m/s)	U_L (m/s)	U_G (m/s)
a	0.31	0.063	0.15	0.80	0.15	0.57	1.38	2.05
b	0.46	0.083	0.15	2.52	0.46	0.78	1.84	2.67
c	0.77	0.081	0.15	4.55	0.77	0.14	2.15	4.52
d	1.38	0.141	0.15	3.10	0.15	2.52	2.45	4.28

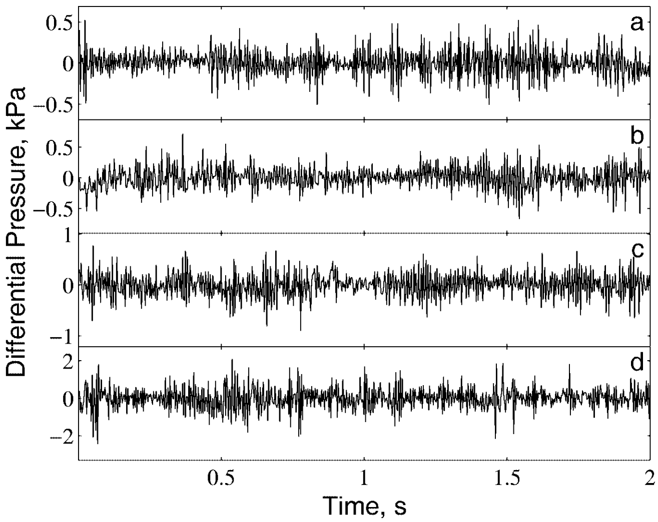

Fig. 2. Differential pressure time series for bubbly flow

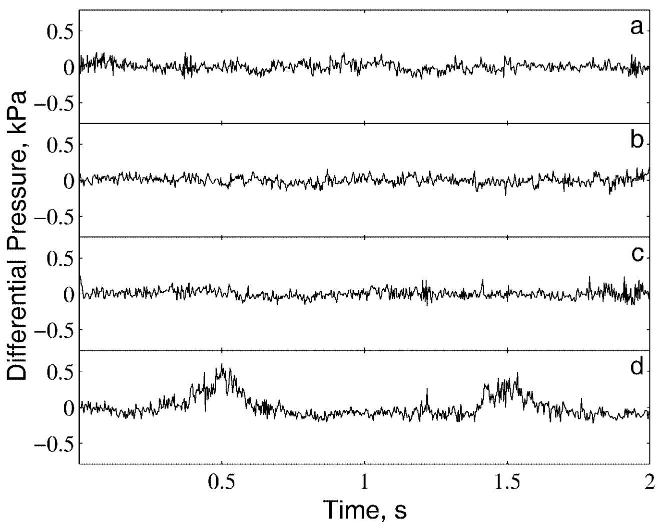

Fig. 3. Differential pressure time series for annular flow

In an annular flow, the gas forms the core at the center of the pipe, and the liquid flows mainly as a film at the wall and partially as droplets in the gas core. When the interface between the gas and the liquid is smooth, a genuine annular flow occurs (Fig. 3a–c). The wavy-annular flow (Fig. 3d), which is a subset of annular flow, is characterized by the presence of large waves on the gas–liquid interface moving with a velocity greater than that of the liquid film. These waves are clearly reflected in the differential pressure time series.

Slug flow is characterized by alternation of large bubbles with a length greater than the pipe diameter (Taylor bubbles) and liquid slugs, either aerated by small bubbles or free of the gaseous phase. By virtue of this intermittent character of the flow, the resulting time series exhibit the features of both bubbly and annular flows.

We observed two kinds of time series characteristic of a slug flow, depending on the relation between the length of the Taylor bubbles and the length of the test section. When the Taylor bubble is longer than the test section, time series (Fig. 4a–b) comprise a sequence of intervals characteristic of annular and bubbly or churn flow separated by an abrupt change in the signal caused by the passage of a Taylor bubble–liquid slug front through the test section. Conversely, if the Taylor bubble length is comparable with the distance between pressure transducers, the signal (Fig. 4c) consists of a sequence of intervals characteristic of bubbly flow broken by waves caused by moving bubbles.

Figure 4d represents the differential pressure signal which is a reflection of a semi-annular flow, characterized by unstable liquid bridges separating the gas core (Spedding et al. 1998). We attributed this flow regime to the slug flow group due to the similar spatial distribution of the phases, that is, alternating regions of low and high gas void fraction.

Churn flow (Fig. 5) exhibits highly disordered distribution of phases in the pipe cross-section as well as along the flow and is characterized by oscillatory motion of the liquid. The differential pressure signal typical of churn flow depicts chaotic fluctuations with a high amplitude.

When the flow conditions are close to the transition boundary between the flow regimes, the flow structure is unstable and patterns characteristic of two flow regimes can be observed at different instants. Thus, for example, the signals shown in Figs. 3b (annular flow) and 4d (slug flow) are fragments of one record with the same mean flow rates of phases (see Table 1).

4 Description of method

Several authors performed spectral analysis of time series associated with natural fluctuations in two-phase flows (see, e.g., Vince and Lahey 1982; Franca et al. 1991; Cai et al. 1996). It was shown that the signal spectral energy distribution can be used as an objective flow regime indicator. However, there are several drawbacks obstructing the usage of the spectral analysis for automatic flow regime identification. The first is that it is difficult to extract a small number of features characterizing the shape of the power spectral density function. The second is that, be-

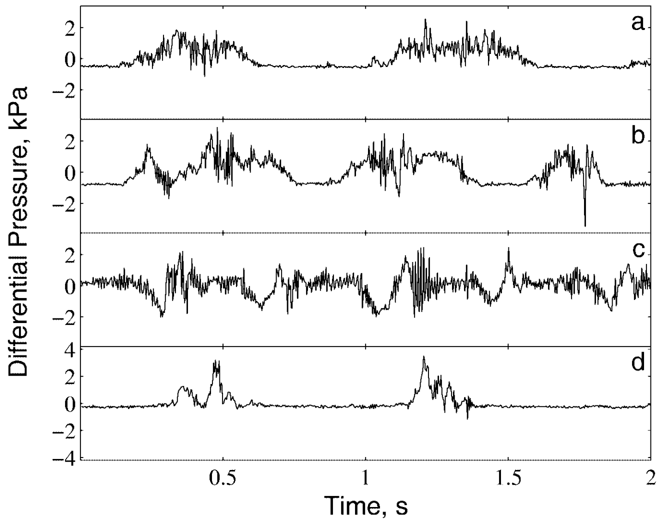

Fig. 4. Differential pressure time series for slug flow

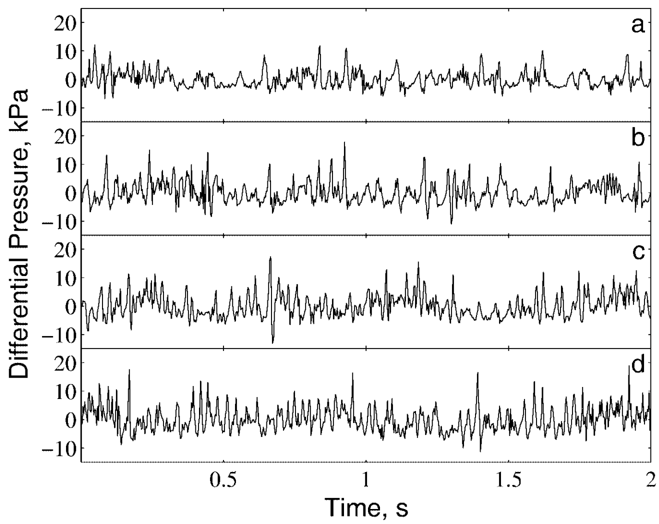

Fig. 5. Differential pressure time series for churn flow

cause of the global character of the Fourier spectrum, the non-stationary nature of the two-phase flows suppresses specific properties of the PSD. Thus, for example, the slug unit length during slug flow varies over a wide range which causes broadening of the PSD peak associated with the slug frequency. Moreover, the accurate estimation of the power spectra with high resolution requires the analyzed signal to be sufficiently long.

The wavelet transform, in contrast, provides time-scale signal decomposition which is intermediate between the time- and frequency-domain representations. Owing to the special properties of the wavelet basis function, it is possible to obtain the local signal energy distribution over the frequency octaves, which provides a small-dimension feature vector characterizing the PSD, and it is useful when the Fourier spectrum is relatively featureless and, hence, can characterize the flow regime. Moreover, the estimates of the spectrum are highly biased, whereas the wavelet spectrum can be effectively estimated even for a moderate length samples (see, e.g., Percival 1995).

Here we present only a brief description of the wavelet transform. Detailed information can be found, for example, in Daubechies (1992) and Meyer (1993). An excellent review of the application of the wavelet transform in fluid mechanics has been written by Farge (1992).

4.1
Discrete wavelet transform

The discrete wavelet transform (DWT) of a square integrable function is defined as its decomposition into an orthogonal set of functions (Mallat 1989)

$$\psi_{jk}(t) = 2^{j/2}\psi\left(2^j t - k\right), \text{ with } j,k \in \mathbf{Z}, \tag{1}$$

which are derived by shifting and scaling the single function $\psi(t)$ called a "mother wavelet". In order to be a wavelet, the function $\psi(t)$ has to satisfy the admissibility condition

$$\int_{-\infty}^{\infty} \psi(t)\mathrm{d}t = 0, \tag{2}$$

and, in order to form an orthonormal basis of $L^2(R)$, it must be orthogonal to its translations $\psi(t\text{–}k)$ and scaled versions $\psi(2^j t)$ for all integers j, k. In addition, the "mother wavelet" must be well localized in both physical and Fourier spaces. Thus, for example, Daubechies (1988) showed that wavelets $\psi(t)$ exist with compact support possessing the properties of a band-pass filter. The coefficients of the wavelet transform of a function $f(t)\in L^2(R)$ are defined as its orthogonal projection onto the wavelet basis:

$$d_{jk} = \int_{-\infty}^{\infty} f(t)\psi_{jk}(t)\mathrm{d}t. \tag{3}$$

Thus, any function $f(t)$ can be decomposed as

$$f(t) = \sum_{j=-\infty}^{+\infty}\sum_{k=-\infty}^{+\infty} d_{jk}\psi_{jk}(t). \tag{4}$$

Owing to the localization properties of the wavelets, the wavelet coefficients d_{jk} can be viewed as the measure of fluctuations of the analyzed function near the time $2^j k$ and in the frequency band whose endpoints are proportional to 2^j, or at the scale 2^{-j}. This property of localization in both time and frequency domains, which are interdependent by the kind of uncertainty principle, turns the wavelet transform into a superior tool for analysis of non-stationary and transient signals.

When dealing with a sampled discrete signal $f(t)$, t=1,2,...,N, which is usually identified with the approximation at the scale 1, the wavelet decomposition reads:

$$f(t) = \sum_k a_{-Jk}\phi_{-Jk}(t) + \sum_{j=-J}^{0}\sum_k d_{jk}\psi_{jk}(t), \tag{5}$$

where $J \le log_2 N$ is the maximum decomposition level, d_{jk} and a_{jk} are termed the detail and approximation coefficients, respectively, at the scale 2^{-j} (or at the level $-j$), and defined as

$$a_{jk} = 2^{j/2}\langle f(t), \phi(2^j t - k)\rangle,\ d_{jk} = 2^{j/2}\langle f(t), \psi(2^j t - k)\rangle, \tag{6}$$

where $\langle,\rangle$ denotes the inner product. $\phi(t)$ is called "scaling function" and possesses the following properties:

$$\int_{-\infty}^{\infty} \phi(t)\mathrm{d}t = 1,\ \int_{-\infty}^{\infty} \phi(t)\phi(t-k)\mathrm{d}t = \delta_{0,k},$$
$$\int_{-\infty}^{\infty} \phi_{jk}(t)\psi_{j'k'}(t)\mathrm{d}t = 0,\ \forall j' \ge j, \tag{7}$$

such that the set of functions $\phi_{Jk}(t)$, $\psi_{jk}(x)$, $j,k \in \mathbf{Z}$, $j \ge J$, constitutes an orthonormal basis for a wide class of functions.

Owing to the orthogonality of the wavelet basis, the wavelet transform is energy conserving, that is

$$\sum_i |(i)|^2 = \sum_j \sum_k |d_{jk}|^2 + \sum_k |a_{-Jk}|^2, \tag{8}$$

which makes it possible to treat the DWT as time-scale energy decomposition in contrast to the frequency decomposition of the Fourier transform.

4.2 The principle of flow pattern recognition

It was shown in Sect. 3 that the physical processes characteristic of particular flow regime are reflected in the differential pressure signal. By virtue of the properties of the coefficients of the wavelet transform, it is conceivable that the wavelet spectrogram, or scalogram, $|d_{jk}|^2$ of the measured signal can be used for distinguishing between the flow patterns. Thus, in a bubbly flow, the wavelet spectrum is expected to be localized at small scales. In an annular flow, the energy of fluctuations is essentially concentrated at small scales and, partially, in the case of wavy-annular flow, at large scales. The slug flow time series exhibit the intermittent wave-like structures which carry most of the energy of the fluctuations. Hence, slug flow is characterized by the spectrum distributed over the range of intermediate scales. Owing to the chaotic behavior intrinsic to churn flow, the energy of the fluctuations must be evenly distributed between the scales.

It must be noted that, owing to the band-pass filter property of the wavelets, a similar qualitative description of the wavelet spectrum for particular flow regime could be obtained by simply summing up the Fourier spectra over the frequency octaves. In order to provide the quantitative description of the wavelet spectrum which can be used as the feature set for pattern recognition, we define, regarding the energy conserving property of the DWT (Eq. 8), the mean local energy density of a signal in a finite time interval $[t_0,t_1]$ at the scale 2^{-j} as

$$E_j = \frac{1}{t_1 - t_0} \sum_{k=2^j t_0}^{2^j t_1} |d_{jk}|^2. \tag{9}$$

It can be shown readily that, for a stationary signal, the mathematical expectation of this quantity is independent of t_0,t_1 and, moreover, for a zero mean signal and a sufficiently large time interval $t_1 - t_0$

$$\sum_j E_j \sim \sum_j \sigma_j^2 = \sigma^2, \tag{10}$$

where σ^2 is the variance of the signal. The quantity σ_j^2 is called the wavelet variance, and the vector of σ_j^2 is referred to as the wavelet spectrum. Equation 10 shows that the wavelet spectrum can be treated as the variance decomposition into scales, in the same way as the power spectral density function is the variance decomposition into frequencies.

4.3 The choice of the analyzing wavelet

The effectiveness of the wavelet analysis strongly depends on the choice of the wavelet basis. The heuristic requirement of the wavelet function is that the original signal can be represented in the most parsimonious way, that is by a small number of essentially non-zero wavelet coefficients which will pick up the fundamental features of the signal and "suppress" the noise. The simple geometric example of the advantages of the best basis is the parsimonious representation of a sphere in the spherical coordinates as compared with the Euclidean coordinate system.

The choice or construction of the optimal wavelet basis is usually accomplished in terms of some preset criterion provided by the statistical information theory, e.g., entropy (Coifman and Wickerhauser 1992) or sparsity (Johnstone 2000). The Shannon entropy of the unit norm vector f is defined as

$$S_f = -\sum_j |f_j|^2 \ln |f_j|^2, \tag{11}$$

and the sparsity is quantified using norms in spaces of finite real sequences:

$$\|f\|_p = \left(\sum_j |f_j|^p\right)^{1/p} \tag{12}$$

for $p<2$, the smaller p, the more pronounced the quality of the representation. The best wavelet basis for a given signal is that for which the specified criterion evaluated for the wavelet decomposition coefficients attains the minimum value.

In our case, it is difficult to choose the wavelet which will compose the best basis for any measured signal because the characteristics of the signal are flow-regime dependent and the wavelet suitable for the slug flow signal, for instance, will not fit the signal measured in a churn flow. Hence, the analyzing wavelet must be chosen to provide the best representation "on average". As for bubbly and annular flows, the representation of the corresponding signals is almost insensitive to the choice of wavelet, since the noise is not sparse on any basis (the Fourier spectrum of the white noise, for example, is evenly distributed over all frequencies).

In order to find a suitable wavelet among the collection of basic well-known wavelets (see Misiti et al. 1995), we compared the sparsity (Eq. 12) of the wavelet representation for the wide set of the experimental time series representing slug and churn flow regimes. Daubechies' least symmetric wavelet of order four (Daubechies 1988), which reduces the sparsity by 40% on average with respect to the time domain representation, was chosen in this study for the analysis of the differential pressure time series.

5
Wavelet decomposition of differential pressure time series

In order to examine the potential of the wavelet transform for flow pattern recognition, we performed an eight-level wavelet decomposition of the 2-s differential pressure time series shown in Figs. 2, 3, 4, and 5. As will be shown further, only the relative distribution of the variance over the scales, and not their absolute values, can be used to interpret the dynamic processes characteristic of particular flow regimes. Therefore, each signal was normalized by its variance before processing. Figures 6, 7, 8, and 9 show the mean local energy density distribution (Eq. 9) for different flow regimes. The ninth coefficient on these plots is the variance of the approximation coefficients at the last level of decomposition (see Eq. 6). This ensures that the total energy is $\sum_j E_j = 1$.

In a bubbly flow, the gas void fraction at a particular pipe section fluctuates around its mean value as bubbles pass through the test section. The stochastic nature of the distribution of bubbles along the flow as well as the turbulent pressure fluctuations in the liquid give rise to the high-frequency signal in which the energy of fluctuations (Fig. 6) is concentrated at scale 2 (first level).

The main source of the void fraction fluctuations in annular flow is the variation in the liquid film thickness, and the inspection of the wavelet energy distribution (Fig. 7a–c) indicates high energy content on the smaller scale. However, contrary to bubbly flow, significant energy of fluctuations is distributed over the higher time scales. This behavior can be explained as follows. The liquid film thickness in an annular flow is distributed in a wide range (see, e.g., Wolf et al. 2001) with a well-defined peak corresponding to the thickness of the film sublayer between two successive disturbance waves. This implies that the largest fraction of energy of the film thickness fluctuations is concentrated at the small ripples. The greater the wavelength of the disturbances (and the associated time scale of the signal), the smaller is their contribution to the energy of fluctuations. However, when a rare long wave with a high amplitude occurs, it causes a considerable decrease in the gas void fraction and a consequent increase in the differential pressure amplified by the acceleration in the Venturi meter. The corresponding wavelet spectrum exhibits high-scale energy distribution (Fig. 7d).

As mentioned above, the time series characteristic of slug flow comprises alternating intervals characteristic of bubbly and annular flow. Such an intermittent time series yields a bimodal probability density function, typical for slug flow (Jones and Zuber 1975; Tutu 1982), one mode corresponding to the liquid slugs and another to the Taylor bubbles. The wavelet spectrum (Fig. 8) also exhibits two peaks. In this case, however, the small-scale peak represents the high-frequency fluctuations of bubbly and annular flows and the second peak, which is spread over the range of intermediate scales, reflects the variation in the signal caused by the passage of a bubble-slug front. It must be noted that the location of this second peak depends on the time the bubble-slug front passes through the test section. As expected, the distribution of the energy of fluctuations clearly shows the separation of characteristic time scales of the processes occurring in the slug flow.

Chaotic fluctuations in the gas void fraction in the churn flow exhibit themselves in the distribution of the main energy of differential pressure fluctuations over the set of small time scales (Fig. 9). The inspection of the

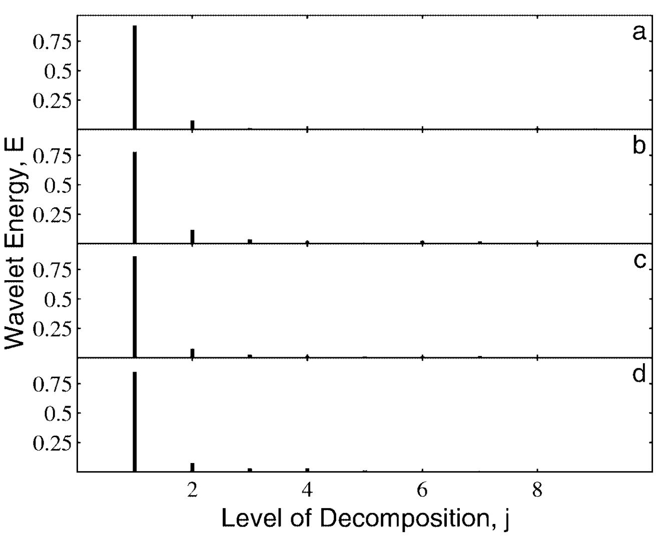

Fig. 6. Wavelet variance distribution over scales for bubbly flow

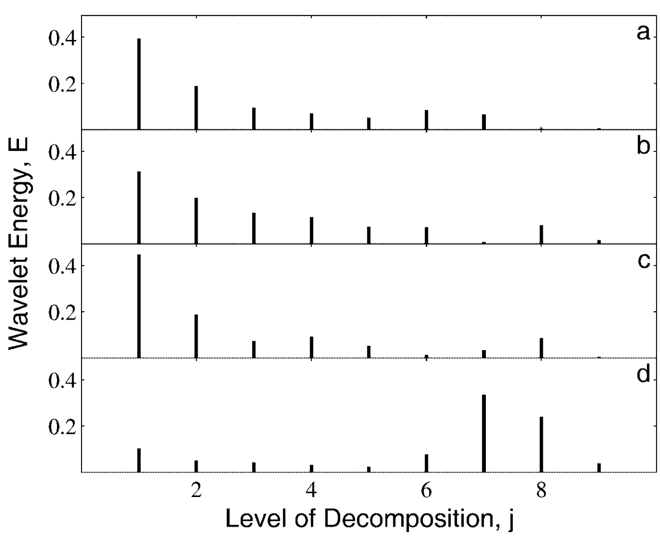

Fig. 7. Wavelet variance distribution over scales for annular flow

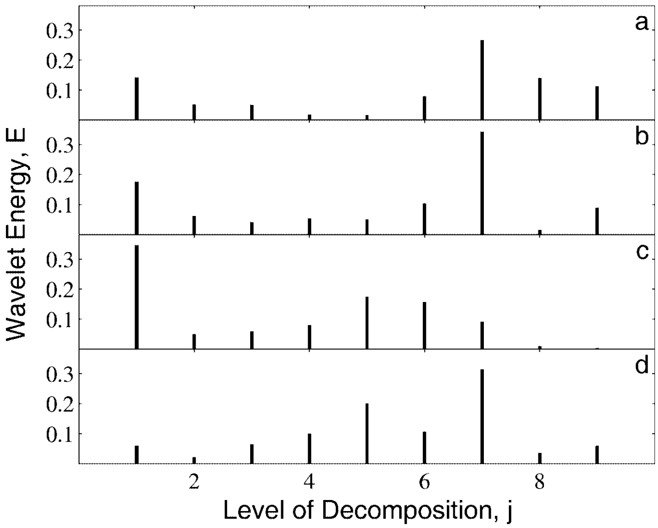

Fig. 8. Wavelet variance distribution over scales for slug flow

behavior of the wavelet variances at the three smallest time scales hints at the existence of universal scaling at high frequencies characteristic for the churn flow. It must be noted that the stochastic signals possessing scaling of the power spectrum, called 1/*f* processes, are usually associated with apparently chaotic processes resulting from a deterministic mechanism, e.g., Brownian motion, turbulence, etc. However, it is difficult to estimate the exact value of the scaling exponent, since there is no separation between the scale at which the data were sampled and the region of interest, and owing to the limited range of frequencies involved (three octaves).

The results obtained here for four different flow regimes evince that the wavelet spectrum of differential pressure time series characterize the dynamic processes specific for particular flow regime and, therefore, can be used for identification purposes. Comparison of the wavelet spectra indicates that the only ambiguity in classifying the flow regime can arise between the slug,

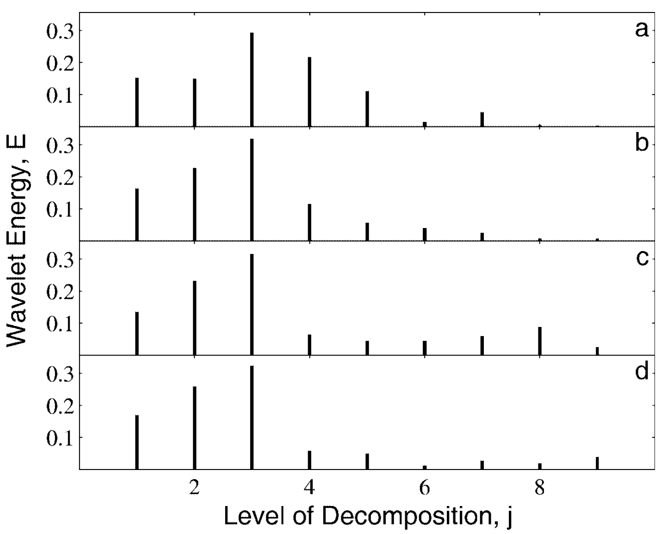

Fig. 9. Wavelet variance distribution over scales for churn flow

semi-annular and wavy-annular regimes (see Figs. 8a–c, d and 7d, respectively). However, a straightforward discrimination between these subregimes can be obtained by observing that the variances of the corresponding time series differ significantly.

Near the transition boundaries between the flow regimes, the flow patterns can change owing to the flow instability. If the analyzed signal is too long in such cases, it will carry features of more than one pattern, and the identification becomes dubious. Matsui (1986) proposed representing the results of identification in terms of probabilities. The method presented implies a different solution to this problem. Since the wavelet transform permits signals with a relatively small length to be analyzed, different segments of the signal will be identified as representing different flow regimes (e.g., annular flow, Fig. 3b, and slug flow, Fig. 4d). In practice, however, one should not chose the signal length too short, since the intrinsic signal transients, such as alternating slugs and Taylor bubbles in slug flow, can be interpreted as flow regime transitions.

6
Summary

The relation between the flow regimes in a two-phase air–water vertical flow and the differential pressure fluctuations measured through the Venturi meter were studied. It was shown that the flow patterns remain stable and unchanged during the flow through the contraction and, therefore, the measured differential pressure contains information reflecting the flow structure and can be used for flow regime identification purposes. The proposed arrangement of the test section has the advantages of being simple and inexpensive as compared with direct void fraction measurement devices, and allows the measurements in two-phase flows to be integrated with a flow regime identification system.

A set of experimental data was analyzed using the wavelet transform. The vector E_j of the distribution of the signal wavelet variance over scales was shown to contain valuable information regarding the hydrodynamic processes characteristic for the two-phase flow regimes studied. Thus, in a bubbly flow, the energy of fluctuations is concentrated at the smallest time scale which reflects the motion of randomly distributed gas bubbles. The fluctuations of the liquid film thickness are expressed as decreasing with scale wavelet variance for an annular flow. The small-scale and intermediate-scale peaks in the wavelet spectrum characteristic of slug flow correspond to the fragments of bubbly or annular flow and intermittent fluctuations, respectively. The chaotic character of a churn flow is manifested by the distribution of the differential pressure fluctuations over the set of small scales.

Using the vector of the distribution of the energy of fluctuations over the scales as the vector of characteristic parameters, it is feasible to classify the time series as being the manifestation of bubbly, annular, churn or intermittent flow. Further classification of the intermittent flow into subgroups can be performed using the value of the regular variance of the measured signal. The exact boundaries between the flow regimes in the feature space can be found using any statistical classifier, for example artificial neural networks.

Two remarkable properties of the wavelet analysis must be noted here. First, a very fast algorithm exists for computing the coefficients of the discrete wavelet transform which requires only $O(N)$ operations, that is faster than the fast Fourier transform. The second is that the estimation of the wavelet coefficients does not require a large sample size, allowing the proposed method to be applied to flow conditions close to the transition boundaries between the flow regimes and to transient flows. Thus, the proposed method can be used for the on-line identification of flow regimes in two-phase systems, and may be implemented with any measurement device provided its output is related to the gas void fraction of the flow.

References

Barnea D, Shoham O, Taitel Y (1980) Flow pattern characterization in two-phase flow by electrical conductance probe. Int J Multiphase Flow 6:387–397

Cai Y, Wambsganss MW, Jendrzejczyk JA (1996) Application of chaos theory in identification of two-phase flow patterns and transitions in a small, horizontal, rectangular channel. J Fluids Eng 118: 383–390

Coifman RR, Wickerhauser MV (1992) Entropy-based algorithm for best basis selection. IEEE Trans Inf Theory 38:713–718

Costigan G, Whalley PB (1997) Slug flow regime identification from dynamic void fraction measurements in vertical air-water flows. Int J Multiphase Flow 23:263–282

Daubechies I (1988) Orthonormal bases of compactly supported wavelets. Commun Pure Appl Math 41:909–996

Daubechies I (1992) Ten lectures on wavelets. CBMS-NSF regional conference series in applied mathematics, vol 61. SIAM, Philadelphia

Farge M (1992) Wavelet transforms and their applications to turbulence. Annu Rev Fluid Mech 24:395–457

Franca F, Acikgoz M, Lahey RT, Clausse A (1991) The use of fractal techniques for flow regime identification. Int J Multiphase Flow 17:545–552

Hubbard MG, Duckler AE (1966) The characterizaton of flow regimes for horizontal two-phase flow. In: Saad MA, Moller A (eds) Proceedings of the 1966 Heat Transfer Fluid Mechanics Institute. Stanford University Press, Stanford, pp 100–121,

Johnstone IM (2000) Wavelets and the theory of non-parametric function estimation. In: Silverman BW, Vasilicos JC (eds) Wavelets, the key to intermittent information? Oxford University Press, New York, pp 89–109

Jones OC Jr, Zuber N (1975) The interrelation between void fraction fluctuations and flow patterns in two-phase flow. Int J Multiphase Flow 2:273–306

Kirpalani DM, Sparks BD, McCracken TW (2001) A wavelet based approach for determining two-phase flow patterns. In: Michelides EE (ed) Proceedings of the 4th International Conference on Multiphase Flow, New Orleans. Tulane University, New Orleans

Mallat SG (1989) Multiresolution approximations and wavelet orthonormal bases of $L^2(R)$. Trans Am Math Soc 315:69–87

Matsui G (1984) Identification of flow regimes in vertical two-phase flow using differential pressure fluctuations. Int J Multiphase Flow 10:711–720

Matsui G (1986) Automatic identification of flow regimes in vertical two-phase flow using differential pressure fluctuations. Nucl Eng Des 95:221–231

Meyer Y (1993) Wavelets. Algorithms and applications. SIAM, Philadelphia

Misiti M, Misiti Y, Oppenheim G, Poggi JM (1995) Micronde: a Matlab wavelet toolbox for signals and images. In: Antoniadis A, Oppenheim G (eds) Wavelets and statistics. Lecture notes in statistics, vol 103. Springer, New York Berlin Heidelberg, pp 239–259

Percival DP (1995) On estimation of the wavelet variance. Biometrika 82:619–631

Soldati A, Paglianti A, Giona M (1996) Identification of two phase flow regimes via diffusional analysis of experimental time series. Exp Fluids 21:151–160

Spedding PL, Woods GS, Raghunathan RS, Watterson JK (1998) Vertical two-phase flow. Part I: Flow regimes. Chem Eng Res Des 76:612–619

Taitel Y (1990) Flow pattern transition in two-phase flow. In: Hetsroni G (ed) Proceedings of the 9th International Heat Transfer Conference, vol 1. Hemisphere, Washington, DC, pp 237–254

Tsoukalas LH, Ishii M, Mi Y (1997) A neurofuzzy methodology for impedance-based multiphase flow identification. Eng Appl Artif Intel 10:545–555

Tutu NK (1982) Pressure fluctuations and flow pattern recognition in vertical two-phase gas–liquid flows. Int J Multiphase Flow 8:443–447

Vince MA, Lahey RT Jr (1982) On the development of an objective flow regime indicator. Int J Multiphase Flow 8:93–124

Wolf A, Jayanti S, Hewitt GF (2001) Flow development in vertical annular flow. Chem Eng Sci 56:3221–3235